Soft Matter

A Comparative Study of Blood Rheology across Species

Journal:	*Soft Matter*
Manuscript ID	SM-PER-02-2021-000258.R1
Article Type:	Paper
Date Submitted by the Author:	28-Mar-2021
Complete List of Authors:	Horner, Jeffrey; University of Delaware, Chemical and Biomolecular Engineering; Sandia National Laboratories, Thermal/Fluid Component Sciences Wagner, Norman; University of Delaware, Chemical and Biomolecular Engineering Beris, Antony; University of Delaware, Chemical and Biomolecular Engineering

ARTICLE

A Comparative Study of Blood Rheology across Species

Jeffrey S. Horner[a,b], Norman J. Wagner[a], and Antony N. Beris[a†]

Received 00th January 20xx,
Accepted 00th January 20xx

DOI: 10.1039/x0xx00000x

Recent advances in hemorheology are extended to study blood rheology across species, which has important clinical implications particularly in intravenous drug scaleup as drugs undergoing clinical trials are first tested in animals. Some of the first hemorheological measurements from seven different species under both steady and transient shear conditions are presented and modeled using a rheological model developed and validated on human blood rheology fit to 20 different donors. Despite similar physiological properties across the blood samples from different species, significant differences are observed, particularly at low shear rates. Blood from species that form rouleaux exhibit a yield-like behavior and enhanced viscoelasticity at low shear rates, while blood from species without rouleaux exhibit nearly Newtonian behavior at similar shear rates. Viscoelasticity due to blood cell deformation is evident for all species at high shear rates. Novel, unidirectional large amplitude oscillatory shear measurements differentiate species. Using the newly acquired data in combination with previous literature data, a new allometric scaling relation is suggested for the low-shear blood viscosity for various mammalian evolutionary orders. Using an established model for arterial branching across species, it is conjectured that the observed hemorheological scaling across species is driven by maintaining a constant wall shear stress in arterial vessels.

1 Introduction

Studying human blood using the tools and methods of soft matter science has proven valuable.[1] Despite significant changes across species in body mass, lifestyle, and anatomy, the physicochemical and biological composition of blood are approximately conserved.[2] Red blood cells (RBCs), the main constituent in addition to plasma, are a common feature to blood for almost all vertebrates. Unlike RBCs from other vertebrates, mammalian RBCs lack nuclei and organelles and are typically biconcave disc shaped, with minor exceptions such as camelid RBCs which are oblate spheroids.[3] When compared to the order of magnitude changes in body mass, the changes in RBC size and volume fraction across species are relatively small and do not show any obvious trend with body mass.[4,5] The evolutionary reason for the biconcave disc shape that RBCs exhibit is still an area of active research with some researchers suggesting that, in addition to maximizing surface area to enhance transport, the shape enhances deformability and improves the flow properties of blood.[6,7]

Human blood has been widely studied and is known to exhibit complex flow effects under pressure-driven flow within microvessels such as the Fahraeus and Fahraeus-Lindqvist effects, a decrease in the local hematocrit and a decrease in the apparent viscosity, respectively.[8,9] Even in the bulk, rheologically, human blood also demonstrates complex behavior including pseudoplasticity, viscoelasticity, and thixotropy.[10–13] These effects arise primarily because of the formation of rouleaux, coin stack structures comprised of RBCs, at low shear rates and in the presence of plasma proteins. Rouleaux formation is not a common feature to all vertebrates or all mammals and will occur to different extents across species. The biconcave disc shape is a requisite condition for rouleaux formation; although, the converse is not always true[13]. Several unsuccessful attempts have been made to correlate the extent of rouleaux formation with physiological properties of blood across species (*e.g.*, hematocrit, fibrinogen concentration, RBC deformability, and RBC surface charge) or with ecological features of the species (*e.g.*, body mass, diet, and aerobic capacity).[14-16] Thus, the question of why rouleaux form in certain species or, equivalently, why the flow behavior of blood varies across species is still open in the field of comparative hemodynamics.

In this work, we present new rheology measurements under steady and, for the first time, transient shear conditions for blood from seven different species (guinea pig, chicken, human, sheep, pig, horse, and cow) using a protocol developed to yield reproducible and accurate measurements of human hemorheology.[17] An established structure-kinetics rheological model developed to describe transient human hemorheology is then successfully fit to the data.[18] A comparison of the model parameters across species provides insight into the mechanistic variation in blood rheology. We conclude with a discussion of the possible evolutionary origins for these significant variations

[a] *Center for Research in Soft Matter and Polymers, Department of Chemical and Biomolecular Engineering, University of Delaware, Newark, DE 19716*
[b] *Current address: Thermal/Fluid Component Sciences Department, Sandia National Laboratories, Albuquerque, NM 87123*
† Corresponding author: Beris@udel.edu
Electronic Supplementary Information (ESI) available: Data and formula used to describe hematocrit dependence; Allometric Branching Model Derivation. See DOI: 10.1039/x0xx00000x

in the rheological properties of blood across species. By combining our steady state results with literature data, we identify a suggestive allometric scaling relation for the low-shear viscosity of blood across species. This work aims to bring further awareness to the significant and complex differences in blood from different species, while providing a biophysical rational for variations across some species. This serves to better understand the evolutionary design of blood across species and how it is optimized to efficiently transport oxygen and other nutrients throughout the body while approximately preserving the same wall shear stress, thus allowing easier adaptation of the endothelium cells covering the vessel walls. Additionally, a scaling relation for blood rheology across species can be important for clinical drug testing in animal models.

2 Results and discussion

2.1 Steady Shear Blood Rheology

Anticoagulated whole blood samples were collected from seven species and the results for the steady shear viscosity measurements are shown in Fig. 1(a). The data shown for human blood are the median measurements for 20 different donors sampled, and the band encompasses one standard deviation from the mean. The most obvious difference across species occurs at the low shear rates. Some species like human, pig, and horse exhibit strong shear thinning behavior here, as evidenced by the sharp decrease in viscosity, while other species like chicken, sheep, and cow exhibit an almost constant viscosity behavior.

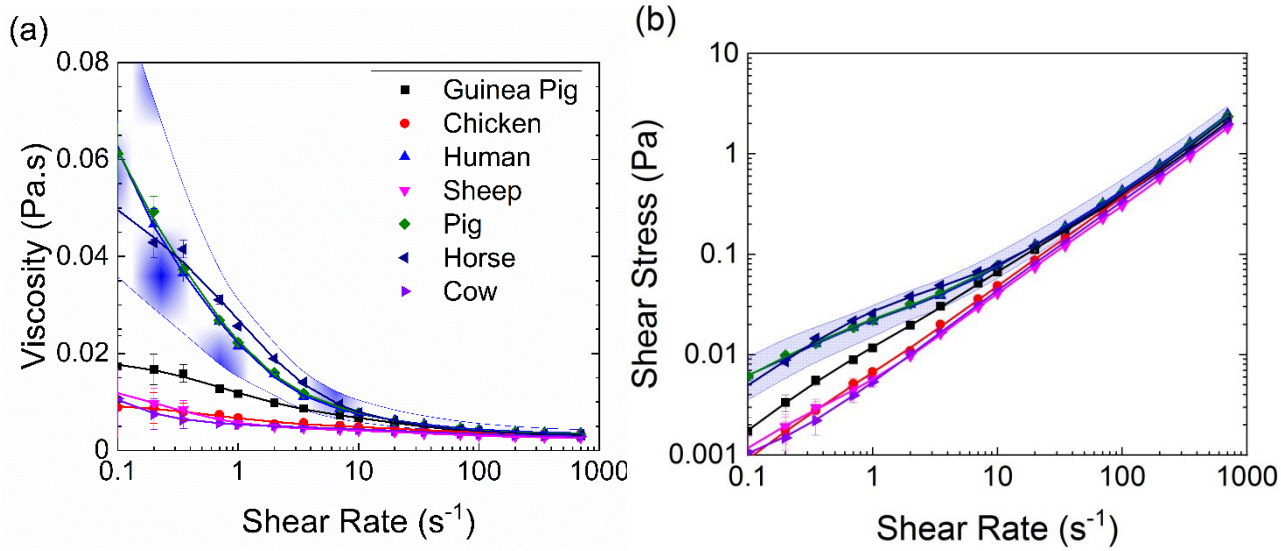

Figure 1. Steady shear stress (a) and viscosity (b) measurements and model fit for blood from various species. Human data points are the median of 20 donors and the bands represent one standard deviation away from the mean.

The differences between species are most clearly appreciated when replotted in Fig. 1(b) as wall stress vs. shear rate. This result is due to the differing aggregation tendency of RBCs in the respective species. For blood from species that exhibits strong shear thinning, the RBCs will form rouleaux at the low shear rates giving rise to this yield-like behavior[10,19]. This yielding behavior corresponds to the aggregate network formed across the rouleaux at stasis which is able to sustain a finite applied stress

Using the steady shear data presented in Fig. 1, a model previously developed for human blood rheology is fit to the data for use in further comparisons: [18]

$$\sigma_{SS} = \left(\frac{\mu_{0,C} - \mu_{\infty,C}}{1 + \tau_C|\dot{\gamma}|} + \mu_{\infty,C}\right)\dot{\gamma} + \mu_R\left(\frac{1}{1 + \tau_b|\dot{\gamma}|}\right)^{1.5}\dot{\gamma} + \sigma_y\left(\frac{1}{1 + \tau_b|\dot{\gamma}|}\right) \quad [1]$$

In Eq. 1, σ_{SS} represents the steady shear stress; $\mu_{0,C}$, $\mu_{\infty,C}$, and μ_R represent viscosities corresponding to the zero shear isolated RBCs, infinite shear isolated RBCs, and the rouleaux, respectively; τ_C and τ_b represent time constants corresponding to the RBC deformation and structural breakdown, respectively; $\dot{\gamma}$ is the shear rate; and σ_y is the yield stress. The respective fits are shown as lines in Fig. 1. Despite the significant difference across species, with several exhibiting viscosities outside of the expected range for human blood, the model is still able to accurately fit the steady shear viscosity for all species. Through the physically meaningful parameters in the model, the changes across species are quantified to develop a better understanding of similarities and differences. This is presented in the form of box and whisker diagrams as shown in Fig. 2. As expected from the experimental data presented in Fig. 1, the rheological properties of blood from guinea pig, chicken, sheep, and cow differ the most from human blood. However, interestingly, several parameters for pig and horse blood also lie more than one standard deviation outside the mean for human blood despite the full steady shear viscosity data for both being

encompassed by this range. It should be noted that the stress components associated with rouleaux formation (σ_C and μ_R) were close to zero for animals whose RBCs do not form rouleaux. As a result, the rouleaux breakage time constant (τ_b) for these animals does not significantly affect the model, and thus, the values have little physical implication. This sensitivity of the model parameters emphasizes the complex, multicomponent nature of blood and necessitates a more thorough understanding of how specific contributions to the bulk rheology of blood change across species.

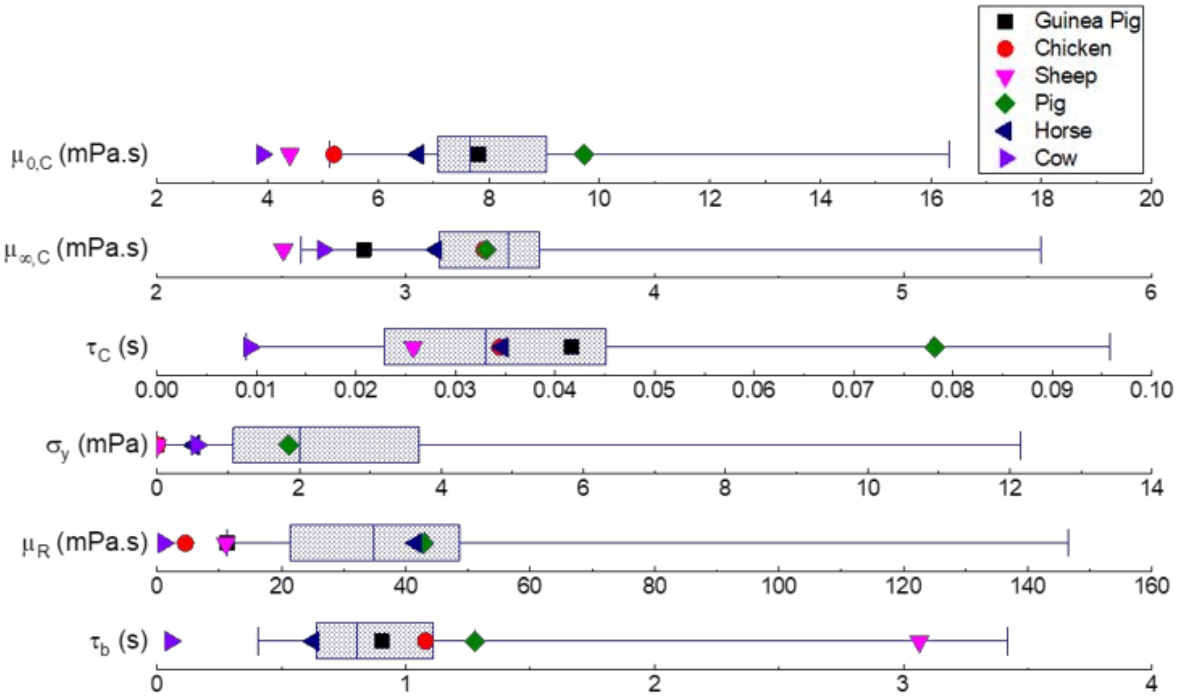

Figure 2. Steady shear rheological model parameters compared to human ranges for 20 donors.

ARTICLE

2.2 Unidirectional Large Amplitude Oscillatory Shear

The subtle changes to the rheology of blood from various species may be better probed through transient shear experiments in addition to steady shear. To best mimic the *in vivo* flow behavior, a pseudo-pulsatile shear waveform test, known as unidirectional large amplitude oscillatory shear (UD-LAOS), was imposed on the sample, given in Eqs. 2 & 3: [13,18]

$$\gamma(t) = \gamma_T(t) + \gamma_o\omega t = \gamma_0 \sin(\omega t) + \gamma_0\omega t \quad [2]$$

$$\dot{\gamma}(t) = \dot{\gamma}_T(t) + \gamma_0\omega = \gamma_0\omega\cos(\omega t) + \gamma_0\omega \ , \quad [3]$$

where γ_0 is the strain amplitude, ω is the frequency, t is the time, and the subscript T denotes the transient strain or shear rate. This test superimposes an oscillatory shear with a steady shear equal in amplitude to the oscillation to prevent flow reversal. The corresponding stress waveforms and effective Lissajous-Bowditch projections at varying frequencies and strain amplitudes are shown in Fig. 3. The aforementioned model for blood rheology features a transient component which has previously been used to fit and predict these experiments for human blood.[13,18] The corresponding fits for the blood samples from all species are also shown in Fig. 3.

Notable differences across species are observed in the UD-LAOS experiments at 1 rad/s and 0.2 rad/s. Particularly, top-bottom asymmetry and a vertical shift are observed in the Lissajous-Bowditch projections for species which exhibit rouleaux formation (*i.e.,* horse, pig, and human). This asymmetry is expected for pseudoplastic fluids, and a vertical shift is indicative of both a yield stress and increased viscoelasticity.[13] By probing the response over varying frequencies and amplitudes, the kinetics of the rouleaux formation can be evaluated, a feature which cannot be properly evaluated with steady shear alone. Despite changes in the low frequency UD-LAOS behavior across species, at 10 rad/s, the behavior of all species is similar. This indicates that rouleaux formation is absent in this regime. Nevertheless, right-left asymmetry and a vertical shift are observed, indicating the presence of viscoelasticity. The presence of viscoelasticity at high frequencies and strain rates can be captured by the model even in the absence of structure and was previously hypothesized to arise from shear deformation of isolated RBCs.[13] This hypothesis is strengthened by these results as the viscoelasticity remains in blood from species without rouleaux.

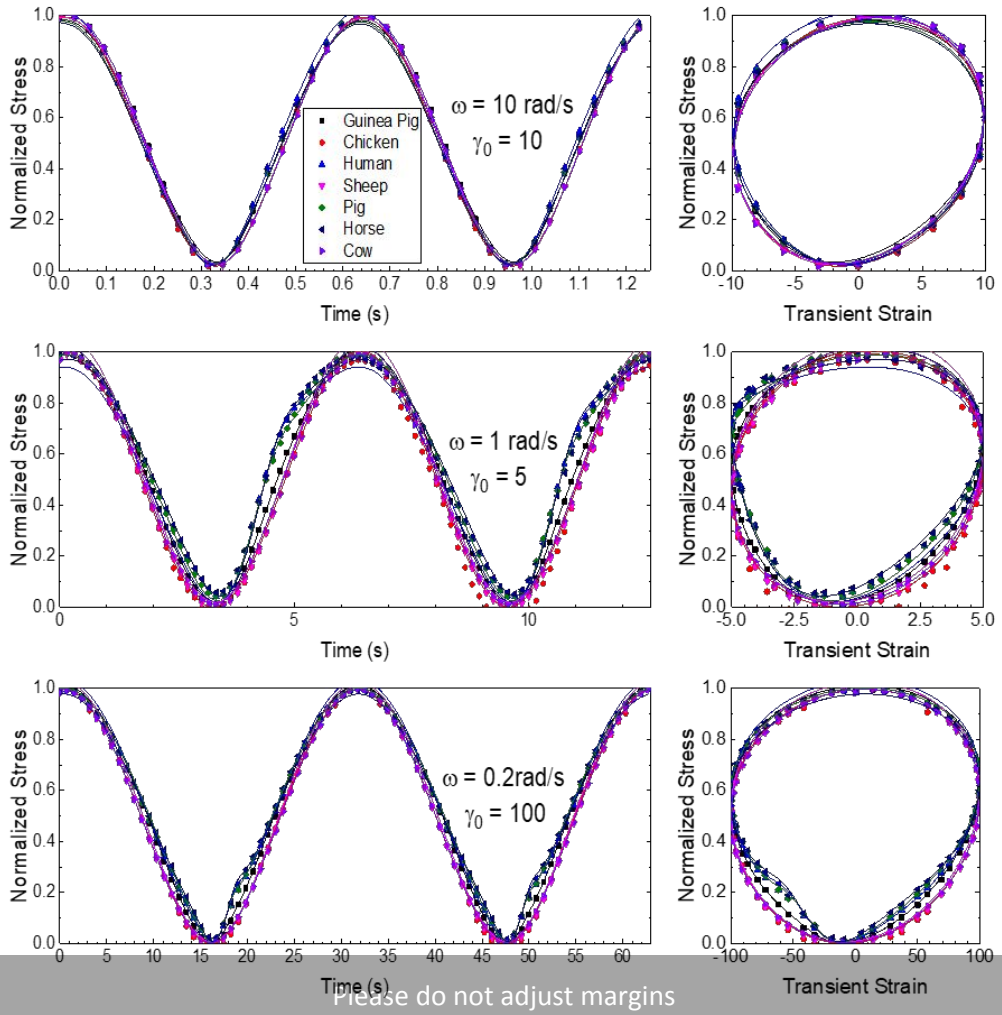

Figure 3. UD-LAOS measurements and model fit for blood from various species. Left figures are the response as a function of time and left figures are effective Lissajous-Bowditch projections (plotted as a function of transient strain). Moving from top to bottom, the tests were completed at a frequency of 10 rad/s and a strain amplitude of 10, a frequency of 1 rad/s and a strain amplitude of 5, and a frequency of 0.2 rad/s and a strain amplitude of 100.

2.3 Blood Syneresis

Thus far, all results presented have been assumed to be under homogeneous conditions. However, previous authors have shown that RBCs are also linked to the Fahraeus-Lindqvist effect, *i.e.*, the decrease in apparent viscosity that occurs when blood flows through small vessels as a consequence of margination and excluded volume effects.[20] This can also occur under conditions of lower shear rates even for larger vessels due to the formation of RBC aggregates (rouleaux) which have larger excluded volumes. As a result, while the bulk viscosity may increase when rouleaux are present, the apparent viscosity for Poiseuille flow may decrease under certain conditions due to this effect. This has been studied experimentally in glass capillaries.[9,22] However, the *in vivo* relevance of the Fahraeus-Lindqvist effect has not been clearly established.[21] For planar shear flow, a similar phenomenon arises, known as syneresis, where a depletion layer will form near the walls of the measurement device at low shear rates.[22] This effect is evident in the experimental data presented in Fig. 4, where blood, previously at a high shear rate (300 s^{-1}), is instantaneously stepped down to a low shear rate (1 s^{-1}). An initial increase in the stress is observed for species with rouleaux formation followed by a longer decay. This is due to the initial build-up of rouleaux followed by the formation of a depletion layer. Sedimentation will also occur more quickly in species with rouleaux formation. However, this will likely manifest over longer time scales due to the long vertical component in the measurement device.

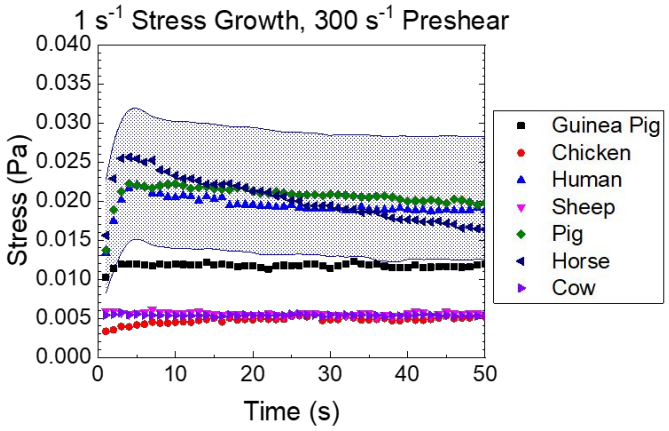

Figure 4. Transient stress measurements at 1 s^{-1} after an instantaneous step down from 300 s^{-1}. Species with rouleaux formation exhibit a long exponential decay in stress corresponding to syneresis.

2.4 Allometric Scaling of Blood Rheology

Our results show that blood from different species can display significantly different rheological responses under flow. The most notable difference arises from the potential presence of rouleaux, which significantly increases the viscosity and viscoelasticity at low shear rates and frequencies. Despite these differences, the previously developed thixotropic model for human hemorheology can capture these variations during both steady shear and UD-LAOS with parameters determined for each species[18]. These observations of different hemorheological behavior across species leads one to question why, from both a physical and an evolutionary standpoint, are these variations observed. Addressing the latter, more comprehensive data are required from a wider range of species to better understand the changes across species and begin to develop a universal scaling relation for interspecies blood rheology. Unfortunately, to the authors' knowledge, sufficiently comprehensive data are not available in the literature. The most comprehensive study for mammals was performed in 1992 by Johnn *et al*. in which the authors measured the viscosity at a single high (128.5 s^{-1}) and low (0.277 s^{-1}) shear rate for a range of species.[23] The low-shear measurements are presented in Fig. 5 as a function of body mass and are colored by evolutionary order.[23-25] Additionally, mammalian measurements from this work are included (shown as open shaded symbols). No apparent correlation of low-shear viscosity with body mass is evident.

Various previous authors have examined allometric scalings for other cardiovascular features across mammals and have shown features scale with body mass according to a power law:

$$Y = Y_{Ref}\left(\frac{M}{M_{Ref}}\right)^{n} \quad , \qquad \textbf{[4]}$$

where Y is some cardiovascular feature, Y_{Ref} is a reference value for that feature, M is the body mass of the mammal, M_{Ref} is the body mass of the reference species, and n is power law exponent.[5] From an initial examination of the experimental data, despite order of magnitude changes in the viscosity, no clear trend with body mass is evident. However, as shown in the previous results, blood can exhibit two significantly different rheological profiles – one which features increased shear thinning associated with rouleaux formation and breakdown and one which features an almost Newtonian behavior with slight shear thinning and viscoelasticity arising only from the deformable nature of isolated RBCs. Moreover, hematocrit fluctuations across individuals can significantly alter the viscosity as has been widely studied for human blood.[11,26,27]

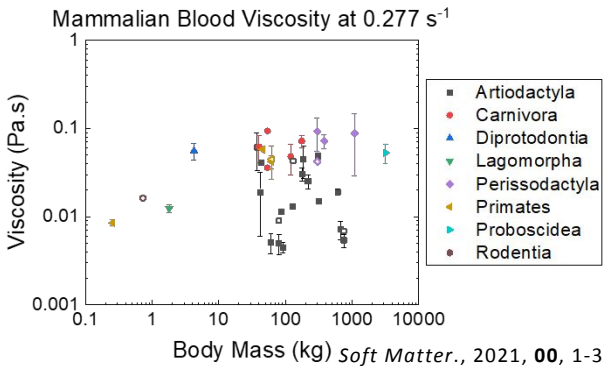

Figure 5. Low-shear (0.277 s^{-1}) blood viscosity measurements from various species colored by evolutionary order. Data from this work are represented as open symbols. All other data is taken from Johnn *et al.*, 1992[23] and Bodey and Rampling, 1998.[24] Reference body mass values were obtained from AnAge: The Animal Ageing and Longevity Database.[25]

Excluding artiodactyla (sheep, pig, and horse for the species sampled in this work), which is the only evolutionary order among those considered here that includes some species with non-biconcave disc RBCs and other species whose RBCs do not form rouleaux, and normalizing by hematocrit, which is relatively constant across species on average, an allometric scaling relation emerges between the low-shear blood viscosity and body mass, as shown in Fig. 6.[23-25] Based on the available data, the scaling exponent is 0.237 ± 0.029 (0.278 ± 0.021 if proboscidea are omitted as an outlier). This is close to a ¼ scaling which has been observed and predicted for numerous cardiovascular features including circulation time, circulation distance, and Womersley number.[28, 29] This ¼ power law scaling is shown as the dashed line and has an R^2 value of 0.812, essentially indistinguishable from the best fit correlation. It is currently unknown why some artiodactyla do not follow this trend. However, this deviation of artiodactyla from allometric relations for hemodynamic parameters for other order has been reported and is thought to originate from an evolution at higher altitudes.[30,31] Exploration into artiodactyla intraorder blood rheology scaling should be a topic of future research as numerous species in this order (*e.g.,* pig, cow, etc.) are used in medical research, and the blood rheology can vary significantly.

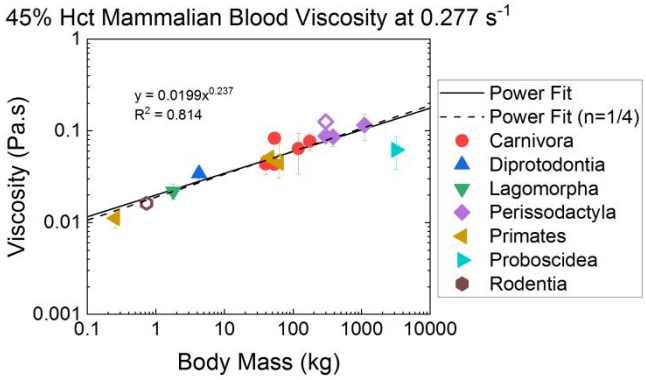

Figure 6. Low-shear (0.277 s^{-1}) 45% hematocrit blood viscosity measurements from various species colored by evolutionary order. Open symbols represent data from this work which were shifted to 45% hematocrit using correlations derived from the remaining Johnn *et al.*, 1992[23] and Bodey and Rampling, 1998[24] data. A power law fit is provided. Reference body mass values were obtained from AnAge: The Animal Ageing and Longevity Database.[25]

2.5 *In Vivo* Wall Shear Stress Predictions

The origin of this new allometric relation for low-shear blood rheology is hypothesized to arise from the requirement of maintenance of wall shear stress across species in vessels where viscous effects are relevant. Scaling of wall shear stress with body mass across species is difficult to measure experimentally and not universally agreed upon.[32] Almost all previous theoretical allometry studies have treated the viscosity of blood as a constant and used the Poiseuille equation to deduce the shear stress, often obtaining negative exponential scaling with body mass in large vessels.[5,33] However, as we have shown in the first portion of this work, blood viscosity is not constant with respect to shear rate nor across species. There are several intuitive arguments that can be made for wall shear stress being independent of body mass, particularly in vessels where viscous effects are important. Namely, endothelial cells have finite stress limits that they can function under. Additionally, platelets and other components in the blood use viscous stresses as biological signals and are only able to operate within small stress windows.[34]

The low shear blood viscosity is relevant mainly in systemic circulation where viscous forces overcome inertial forces. For *in vivo* behavior, this is quantified through the Womersley number (α):

$$\alpha = r\left(\frac{\omega\rho}{\mu}\right)^{\frac{1}{2}}, \qquad \textbf{[5]}$$

where r is the radius of the vessel, ω is the pulse frequency, ρ is the density of blood, and μ is the viscosity of blood.[35] It should be noted that this expression assumes a constant viscosity for blood. As shown in Fig. 1, if the shear rate is sufficiently high (>10 s^{-1}), the infinite shear viscosity can be used as a reasonable approximation. However, viscous effects become relevant at values of the Womersley number below 1.[36] Thus, to identify the clinical significance of the changes in rheology across species, one should look to vessels with $\alpha \leq 1$. A branching model previously proposed by West and coworkers [28] can be used to deduce the body mass dependence of the fluid mechanical parameters governing circulation in these vessels, according to the derivation presented in the SI Appendix. For a characteristic branch level ($k = k_{\alpha=1}$) where viscous effects become relevant, one finds that the apparent wall shear rate has an expected scaling exponent of –0.055.

Linking the previously observed low-shear viscosity scaling to the characteristic shear rate in small vessels scaling is not trivial. As blood is non-Newtonian and the *in vivo* flow is Poiseuille-like, both the viscosity and shear rate are changing across the vessel diameter. Thus, a constitutive model is needed to describe the viscosity changes with respect to shear rate. Unfortunately, due to the lack of available data, the proposed model in the first portion of this work has more parameters than data points available (*i.e.,* only one data point available at 0.277 s^{-1}). However, a widely used generalized Newtonian model for blood, the Casson model:

$$\sigma^{\frac{1}{2}} = \sigma_y^{\frac{1}{2}} + (\mu\dot{\gamma})^{\frac{1}{2}}, \qquad \textbf{[6]}$$

features only two parameters, the yield stress (σ_y) and the infinite shear viscosity (μ).[37] The infinite shear viscosity is widely agreed to be independent of body mass as it is most strongly dependent on hematocrit, another body mass independent

variable. This leaves a single parameter, the yield stress, which can be determined from the low-shear (LS) viscosity scaling relation (*i.e.,* $\eta_{LS} = \eta_{LS,Ref}(M/M_{Ref})^n$). For Poiseuille flow, the wall shear stress (σ_w) for a Casson fluid can be evaluated implicitly according to:

$$\frac{\overline{u}}{r} = \frac{\sigma_w}{4\mu}\left(1 - \frac{1}{21}\left(\frac{\sigma_y}{\sigma_w}\right)^4 - \frac{16}{7}\left(\frac{\sigma_y}{\sigma_w}\right)^{\frac{1}{2}} + \frac{4}{3}\left(\frac{\sigma_y}{\sigma_w}\right)\right), \quad [7]$$

as solved by Apostolidis and Beris.[11] Using hemodynamic reference values for humans, this expression is solved for σ_w in the aorta ($k = 0$) and at $k = k_{\alpha=1}$ in Fig. 7 at varying values of the low-shear viscosity power law scaling exponent (n).[5,38,39]

This analysis demonstrates that if wall shear stress is to be maintained in blood vessels across species, the power law exponent relating low-shear blood rheology and body mass should be positive and around 0.25 (green line in Fig. 7a,b), which is what is approximately observed experimentally as shown in Fig. 6. For aortic flow, an increase in the wall shear stress is observed for smaller species reflecting the diminishing influence of blood yield stress scaling at low body masses. However, aortic flow is dominated by inertia, especially for larger species where flow may even be turbulent and the derived relations for the wall shear stress are not accurate. Thus, it is more important to look to vessels where viscous effects are more relevant (*i.e.,* smaller values of α). Looking to this region and normalizing across species by α, one can see a flatter plateau of the wall shear stress as predicted by the Casson model with a 0.25 exponent for the low shear viscosity. Although an exact scaling is difficult to identify because the analysis involves numerous simplifications and assumptions, the negative scaling of apparent wall shear rate with body mass necessitates a positive scaling of low shear viscosity with body mass to maintain a constant wall shear stress.

It should be noted that this is an oversimplified approach neglecting Fahraeus-Lindqvist effects and normal stresses, that also uses viscosity at one shear rate, and applies a viscosity model that has only been applied to human blood with human reference parameters which can affect the overall results. There is also an upper limit to blood viscosity, as at higher viscosity (and equivalently higher rouleaux formation) the RBCs will sediment out of suspension faster. Lastly, this analysis is only valid at vessels above the critical branch point, $k = \overline{k}$, where branching transitions from area preserving (*i.e.,* da Vinci's rule) to apparent shear rate preserving (*i.e.*, Murray's law).[28,33,40] Beyond this point, the flow is typically considered to be independent of body mass. We hypothesize that this transition could occur around the point at which the flow is no longer governed by the bulk properties of blood but is instead governed by the individual RBC properties. Nonetheless, the simplified analysis shown here strongly supports that hypothesis that the empirical allometric scaling identified in this research that is presented in Fig. 6 is a natural and intuitive biophysical consequence of maintaining a constant wall shear stress. Further research is warranted to explore this promising result further as well as the apparent deviations for some species in the order artiodactyla.

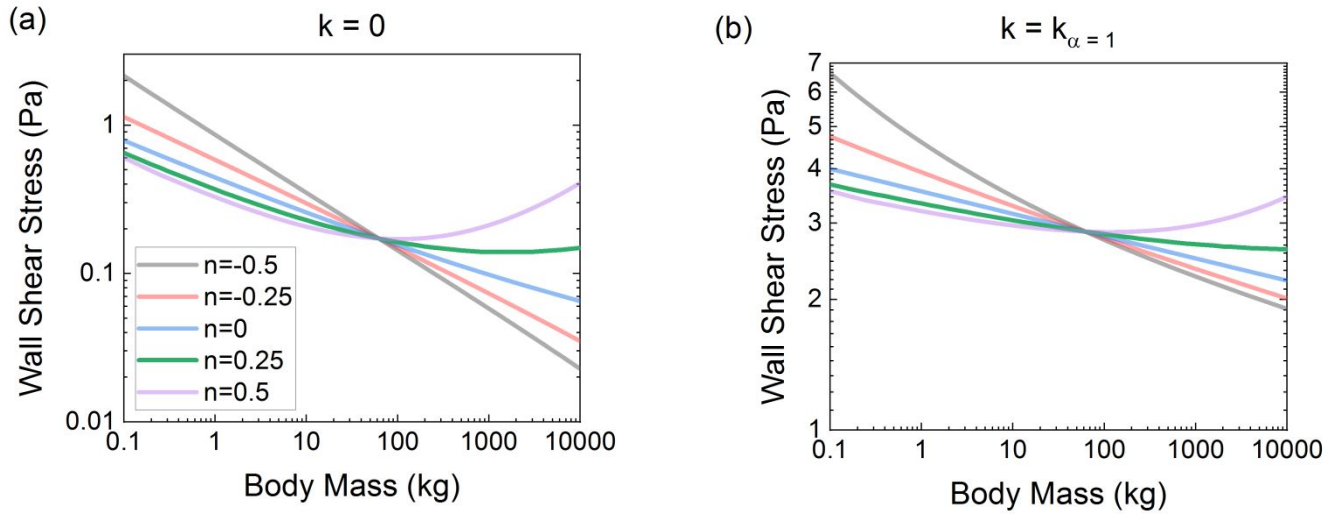

Figure 7. Casson model predicted wall shear stress in the aorta (a) at $k = k_{\alpha=1}$ (b) as a function of body mass. Various values of the low-shear (0.277 s^{-1}) viscosity allometric scaling exponent (n) are shown

3 Conclusions

The first, systematically obtained, hemorheological measurements from across different species covering both steady and transient shear conditions are compared against an extensive data base for human hemorheology. A thixotropic rheological model, previously developed to describe human blood rheology, can equally fit all the animal experimental data. These fits and the resultant parameters with uncertainties, enable a systematic comparison of the complex hemorheology across species, with the significance of variances evaluated

against the variance obtained across 20 human subjects. Statistically significant differences are observed, despite similar physiological properties across the blood samples from different species.

Regarding general hemorheological behavior, we showed that blood from species that form rouleaux exhibit a non-zero yield stress and an enhanced viscoelasticity at low shear rates, while blood from species without rouleaux exhibit nearly Newtonian behavior at similar shear rates. In contrast, viscoelasticity due to blood cell deformation is evident for all species at high shear rates. We also demonstrated how unidirectional large amplitude oscillatory shear can differentiate between these two unique profiles. In addition, using the newly acquired data in combination with previous literature data, a new allometric scaling relation has been discovered for the low-shear blood viscosity for various mammalian evolutionary orders. Moreover, using a previously developed model for arterial branching across species, we showed that such an allometric relation if it exists can help to sustain a constant wall shear stress in arterial vessels. While this proposed allometric scaling is supported by the available data as well as expected based on known physiological properties of arterial branching and principles of fluid mechanics, the significant, but still restricted amount of available hemorheological data under the desired conditions, suggests that additional measurements are warranted to fully validate the observed scaling.

4 Methods

4.1 Blood Collection

Human blood samples were collected according to a previously established procedure for measuring blood rheology.[17] The samples were drawn from the antecubital vein via a 21 G needle into Vacutainer tubes containing 1.8 mg/dL ethylenediaminetetraacetic acid (EDTA). All donors were in the seated position during withdrawal and had previously undergone 8-10 hour fasting. Immediately upon withdrawal, the samples were transported at room temperature and inserted into the double wall concentric cylinder geometry within 30-45 minutes of withdrawal. None of the sampled donors contained known health issues, and donors ranged in age from 19 to 44. For all human blood samples, a complete blood count, lipids panel, and fibrinogen activity test were obtained through Quest Diagnostics.

Animal samples (Lampire Biological Products) were anticoagulated with EDTA. Samples were measured using their native physiological conditions. For all animal blood samples, only the hematocrit was obtained through Lampire Biological Products. Prior to measurement, animal blood samples were cooled to ~4 °C and were transported and inserted into the double wall concentric cylinder geometry within 2.5 hours from withdrawal. In contrast to the human samples, the animal samples were cooled during transit as previous guidelines have shown that cooling helps to prolong the samples if they cannot be immediately measured.[41] However, the cooled samples were given ample time (~45 minutes) to rewarm to the native body temperature before measurement.

4.2 Rheological Measurements

All samples were measured using an ARES-G2 strain-controlled rheometer from TA Instruments equipped with a double wall concentric cylinder geometry (0.5 mm outer gap, 0.43 mm inner gap). A solvent trap was used to prevent sample drying. Temperature was maintained at the native body temperature of the species (all 39 ± 2 °C) to within 0.1 °C using a Peltier temperature controller. The minimum stress for the instrument and geometry is 0.6335 mPa. Prior to each measurement, a preshear of 300 s^{-1} was applied for 30 s. The minimum sampling interval for steady shear data points was 1 s and the minimum sampling interval for transient shear data points was 0.02 s. For the steady shear measurements, reported values at shear rates below 2 s^{-1} correspond to the maximum of the transient measurements to mitigate effects of syneresis. At shear rates above 2 s^{-1}, the reported steady shear values correspond to the average of the final 15 s of measuring.

All measurements were completed within 4 hours of withdrawal. Consistent with our previous work, we expect the variations in the rheological data to be <10 %. These variations correspond to the aggregate effects of sample aging, protein adsorption to free surfaces, and sedimentation[17]. Sedimentation and protein adsorption were further mitigated through the selected geometry which features minimal free surface area and a relatively long vertical component. Furthermore, to account for these effects, UD-LAOS stress measurements were shifted according to changes in the preshear from initial measurements (typically < 5%).

4.3 Rheological Model Fitting

The rheological model was fit to experimental measurements using 10 parallel runs of a highly efficient and accurate parallel tempering algorithm.[42] All steady shear parameters were first fit simultaneously to the steady shear flow curve. After this, these parameters were held constant while the remaining transient parameters were fit simultaneously to the three UD-LAOS experiments. The objective function (F_{obj}) to be minimized was defined as the L2 norm of the reduced stress residuals normalized by the average stress of the particular data set (each steady shear point was considered its own data set) as:

$$F_{obj} = \frac{1}{N}\sum_{k=1}^{N}\frac{1}{P_k}\frac{\|\sigma_{model} - \sigma_{data}\|_{2,k}}{\bar{\sigma}_{data,k}}, \quad \textbf{[8]}$$

where N is the total number of data sets to be fit, P_k is the number of points for a particular data set, and σ_{model} and σ_{data} are the stresses predicted by the model and measured experimentally, respectively. For the allometric scaling analysis, the new data were predicted at 0.277 s^{-1} through a linear interpolation of adjacent points. Although all measurements were taken at the native hematocrit of the donor, corresponding values at 45% hematocrit were predicted through an empirical power law fit based on the data reported by Johnn *et al*..[23]

Author Contributions

J.S.H. conducted experiments and modeling; N.J.W. and A.N.B. designed the study; and J.S.H. wrote the manuscript with input from all authors.

Conflicts of interest

There are no conflicts to declare.

Acknowledgements

Funding was provided by the National Science Foundation through CBET 1510837 and by the Delaware Space Grant College and Fellowship Program through NASA Grant NNX15AI19H. We also acknowledge the Nurse Managed Primary Care Center, University of Delaware (UD) STAR campus for support in drawing the human blood samples, Quest Diagnostics for performing the lab tests on human samples, the UD Environmental Health & Safety dept. for assistance in transporting the samples, and Lampire Biological Products for support in drawing the animal blood samples and testing the hematocrit. We thank Dr. Donna S. Woulfe (UD) for assistance with sample collection, Dr. Yu-Jiun (Nate) Lin (UD) for discussions and blood sample imaging, Dr. Matthew J. Armstrong at the U.S. Military Academy for assistance in rheological modeling, and Willow Bowen at Stanford Univ. for assistance in obtaining measurements.

Online Supplementary Information

Numerical tables of all of the data presented in this manuscript obtained by the authors is presented online:

https://sites.udel.edu/wagnergroup/files/2016/06/Horner-Thesis-Data.xlsx

Notes and references

1. A. N. Beris, in *Theory and Applications of Colloidal Suspension Rheology*, ed. N. J. Wagner and J. Mewis, Cambridge University Press, Cambridge UK, 2021, Ch. 8 Hemorheology, 316-351.
2. D. J. Weiss and K. J. Wardrop, ed., *Schalm's Veterinary Hematology,* John Wiley & Sons, New York, 2011.
3. J. W. Harvey, *Atlas of Veterinary Hematology*, WB Saunders Company, Philadelphia: 2001.
4. V. M. Savage *et al.*, *Proc. Natl. Acad. Sci. U.S.A.,* 2007, **104**, 4718–4723.
5. K. Schmidt-Nielsen, *Scaling: Why is Animal Size so Important?*, Cambridge University Press, Cambridge, 1984.
6. P. B. Canham, *J. Theor. Biol.,* 1970, **26**, 61–76.
7. C. Uzoigwe, *Med. Hypotheses,* 2006, **67**, 1159–1163.
8. R. Fahraeus, *Physiol. Rev.,* 1929, **9**, 241–274.
9. R. Fahraeus and T. Lindqvist, *Am. J. Physiol.,* 1931, **96**, 562–568.
10. G. R. Cokelet et al., *Trans. Soc. Rheol.,* 1963, **7**, 303–317.
11. A. J. Apostolidis and A. N. Beris, *J. Rheol*., 2014, **58**, 607–633.
12. G. B. Thurston, *Biophys. J.,* 1972, **12**, 1205-1217.
13. J. S. Horner, M. J. Armstrong, N. J. Wagner and A. N. Beris, *J. Rheol.,* 2018, **62**, 577–591.
14. O. Baskurt, B. Neu and H. J. Meiselman, *Red Blood Cell Aggregation*, CRC Press, Boca Raton, 2011.
15. U. Windberger and O. K. Baskurt, in *Handbook of Hemorheology and Hemodynamics*, ed. O. K. Baskurt, M. R. Hardeman, M. W. Rampling and H. J. Meiselman, IOS Press, Amsterdam, 2007, Comparative Hemorheology, 267–285.
16. E. H. Eylar, M. A. Madoff, O. V. Brody and J. L. Oncley, *J. Biol. Chem.,* 1962, **237**, 1992–2000.
17. J. S. Horner, A. N. Beris, D. S. Woulfe and N. J. Wagner, *Clin. Hemorheol. Microcirc.* 2018, **70**, 155-172.
18. J. S. Horner, M. J. Armstrong, N. J. Wagner and A. N. Beris, *J. Rheol.,* 2019, **63**, 799-813.
19. U. Windberger, A. Bartholovitsch, R. Plasenzotti, K. J. Korak and G. Heinze, *Exp. Physiol.,* 2003, **88**, 431–440.
20. W. Reinke, P. Gaehtgens and P. C. Johnson, *Am. J. Physiol. Heart Circ. Physiol.,* 1987, **253**, H540–H547.
21. A. R. Pries *et al.*, *Circ. Res.,* 1994, **75**, 904–915.
22. G. R. Cokelet, J. R. Brown, S. L. Codd and J. D. Seymour, *Biorheology,* 2005, **42**, 385–399.
23. H. Johnn, C. Phipps, S. Gascoyne, C. Hawkey and M. W. Rampling, *Clin. Hemorheol. Microcirc.,* 1992, **12**, 639–647.
24. A. R. Bodey and M. W. Rampling, *Clin. Hemorheol. Microcirc.,* 1998, **18**, 291–298.
25. Human Ageing Genomic Resources, Data from "AnAge: the animal ageing and longevity database." Available at https://genomics.senescence.info/species/. (accessed March 2021).
26. R. E. Wells and E. W. Merrill, *J. Clin. Invest.,* 1962, **41**, 1591–1598.
27. S. Chien, S. Usami, H. M. Taylor, J. L. Lundberg and M. I. Gregersen, *J. Appl. Physiol.,* 1966, **21**, 81–87.
28. G. B. West, J. H. Brown and B. J. Enquist, *Science,* 1997, **276**, 122–126.
29. J. R. Banavar *et al.*, *Proc. Natl. Acad. Sci. U.S.A.,* 2010, **107**, 15816–15820.
30. D. E. L. Promislow, *Physiol. Zool.,* 1991, **64**, 393–431.
31. O. K. Baskurt and H. J. Meiselman, *Clin. Hemorheol. Microcirc.,* 2013, **53**, 61–70.
32. C. R. White and R. S. Seymour, *Proc. Natl. Acad. Sci. U.S.A.,* 2003, **100**, 4046–4049.
33. R. S. Seymour, Q. Hu, E. P. Snelling and C. R. White, *J. Exp. Biol.,* 2019, **222**, jeb199554.
34. M. LaBarbera, *Science,* 1990, **249**, 992–1000.
35. J. R. Womersley, *J. Physiol.,* 1955, **127**, 553–563.
36. K. Rohlf and G. Tenti, *J. Biomech.,* 2001, **34**, 141–148.
37. N. Casson, in *Rheology of Disperse Systems*, ed. C. C. Mill, Pergamon Press, London, 1959, A flow equation for pigment-oil dispersions of the printing-ink type, 84–104.
38. W. W. Nichols, M. O'Rourke and C. Vlachopoulos, *McDonald's Blood Flow in Arteries: Theoretical, Experimental and Clinical Principles,* CRC Press, Boca Raton, 6th ed., 2011.
39. J. P. Holt, E. A. Rhode and H. Kines, *Am. J. Physiol. Regul. Integr. Comp. Physiol.,* 1981, **241**, R100-R104.
40. C. D. Murray, *Proc. Natl. Acad. Sci. U.S.A.,* 1926, **12**, 207–214.
41. O. K. Baskurt *et al.*, *Clin. Hemorheol. Microcirc.,* 2009, **42**, 75–97.
42. M. J. Armstrong, A. N. Beris and N. J. Wagner, *AIChE J.,* 2017, **63**, 1937–1958.